Initial stage of thermal oxidation of the Si(111)-(7×7) surface

M. Tabe
Atsugi Electrical Communication Laboratories, Nippon Telegraph and Telephone Corporation, 3-1, Morinosato Wakamiya, Atsugi-shi, Kanagawa, 243-01 Japan

T. T. Chiang, I. Lindau, and W. E. Spicer
Stanford Electronics Laboratories, Stanford University, Stanford, California 94305
(Received 27 January 1986)

We report a systematic study of the early oxidation process in a wide temperature range (20—700 °C) for the Si(111)-(7×7) annealed surface. Oxygen uptake data obtained by Auger-electron spectroscopy indicate that the surface oxygen uptake increases and then gradually saturates with O_2 exposure at 20 °C. At intermediate temperatures, there is no saturation and the oxygen uptake rate is enhanced. At 700 °C, the uptake rate is enhanced in the high-exposure (or high-O_2-pressure) region, but is significantly reduced in the low-exposure region, presumably because of oxygen desorption as volatile SiO. Low-energy electron diffraction pattern transition from 7×7 to no pattern through a 1×1 intermediate pattern seems to be governed only by the amount of surface oxygen at any temperature. Using photoelectron spectroscopy we found that O_2 exposures corresponding to this 1×1 pattern result in the disappearance of surface states centered about 0.6 eV below the valence-band maximum. A chemical-shift study of the Si 2*p* core level shows that not only the oxygen uptake rate, but also the way oxygen bonds to Si is strongly dependent on temperature. Our results show that at room temperature (20 °C) all the Si atoms are oxidized at more or less the same rate, so that the adsorbed oxygen atoms are spread out uniformly over the entire Si surface. At high temperatures, certain Si atoms are being oxidized faster (i.e., have more oxygen atoms bonded to them) than others, so that the distribution of adsorbed oxygen atoms is highly nonuniform; we find microscopic regions of SiO_2-like material interdispersed with regions of Si-like material. Therefore, in the early stage of oxidation, heating the substrate causes nonuniform oxidation with microscopic phase separation of SiO_2 and Si in the oxide film. Tight-binding calculations reported in the literature predict the oxygen 2*p* orbital to produce these valence states: O π (nonbonding), O σ (σ bonding), and O *i* (intermediate nature between nonbonding and σ bonding). By studying the O *i*—O π peak height ratio as a function of oxidation temperature and referring to theoretical calculations, we again come to the conclusion of nonuniform oxidation at high temperatures.

I. INTRODUCTION

The Si-SiO_2 interface is interesting both because of the commercial and technological importance of semiconductor devices and because of interest in fundamental understanding of oxidation. Studies of the initial stage of Si oxidation can help us understand the atomic arrangement and electronic structure at this important interface as well as shed new insights into the oxidation process.

Previous early-oxidation studies have concentrated on room-temperature oxidation.[1–9] In room-temperature oxygen adsorption, it is generally accepted that there are two different adsorption steps: a fast and a slow adsorption step. In the fast adsorption step various models on the bonding configuration of the adsorbed-oxygen—Si system have been proposed, and there has been a long controversy over whether oxygen is adsorbed molecularly[3,4,6,8] or atomically.[2,5,7]

Ibach *et al.*[10] reported that they found both atomic and molecular species for less than 10^2 L O_2 [1 L (1 langmuir) $\equiv 10^{-6}$ Torr sec] and only atomic species for greater than 10^2 L O_2 at room temperature. Recently, Hollinger and Himpsel[11] reported that even at monolayer coverage several different bonding geometries coexist so that modeling for a single atomic or molecular configuration is inappropriate. Thus, although the various models seem to contradict each other, it is likely that coexistence of several geometries is complicating the problem. The slow adsorption step is also not well understood, but is generally recognized as the penetration of the oxygen atoms below the Si surface atom layer.[9]

At elevated temperatures, much less information is available for initial oxidation in spite of the technological importance. Enhancement of oxidation and possible bonding geometry have been reported only at 700 K.[10] According to annealing experiments done after room-temperature adsorption,[11,12] the shifted Si 2*p* component moves further toward higher binding energy, indicating change in configuration toward SiO_2. Similarly, Hollinger *et al.*[13] reported that deposited SiO films show the evolution of the chemical structure from a metastable random bonding phase (uniform distribution of oxygen atoms) to a microscopic mixture of Si and SiO_2 (dimensions of SiO_2-like regions are on the order of 10 Å) when the temperature increases. Therefore, a similar trend may be expected for oxidation at elevated temperatures in addition to enhancement of oxygen uptake.

In this paper, we present a systematic study of initial

oxidation of Si(111)-(7×7) surface in a wide temperature range using Auger-electron spectroscopy (AES), low-energy electron diffraction (LEED), and soft x-ray and ultraviolet photoelectron spectroscopy (PES). The amount of oxygen uptake is monitored by the $I(\mathrm{O}(KLL))/I(\mathrm{Si}(LVV))$ Auger intensity ratio for a series of O_2 exposures at each temperature. The surface crystalline periodicity is observed with LEED. The atomic bonding arrangement changes during oxidation is monitored by the evolution of Si $2p$ core level excited with synchrotron radiation from the Stanford Synchrotron Radiation Laboratory (SSRL) and by the systematic change in the O i (intermediate nature between nonbonding and σ bonding) and O π (nonbonding) valence states excited with uv light from a He lamp. The main goals are the following: (1) to obtain general information on the amount of oxygen uptake as a function of O_2 exposure and Si substrate temperature during exposure, (2) to gain information on the temperature dependence of the way oxygen bonds to Si through the analyses of Si $2p$ core-level chemical shifts and O i and O π peak heights.

In Sec. II the experimental procedures used in this study will be described. In Sec. III we present the results (AES, LEED, and PES) and their physical interpretations. Following that is the discussion section (Sec. IV) and possible atomic bonding geometries will be proposed.

II. EXPERIMENTAL

The experiments were performed using a standard UHV chamber which is equipped with a Physical Electronics 15-255 double-pass cylindrical mirror electron energy analyzer, a four-grid LEED optics, a glancing-angle Auger electron gun, an ion bombardment gun for sputter cleaning and a sample manipulator. The light source for Si $2p$ PES was synchrotron radiation from the 4° branch line of beam line I at SSRL, while the light source for valence states PES was monochromatized He I (21.2 eV) light.

The sample used was a piece of degenerately doped (As dopant) n-type Si wafer oriented in the ⟨111⟩ direction. The sample was mounted on a Mo plate and heating of the sample was accomplished by electron bombardment on the back side of the Mo plate using a grill-shaped tungsten filament. The Si surface temperature was monitored by a (W + 5 at. % Re)–(W + 26 at. % Re) thermocouple wire which was pinned by a Mo clip. Initially, the Si surface was cleaned by Ne sputtering with subsequent high-temperature anneal (~1000 °C). Two sputter-anneal cycles yielded a clean Si surface as evidenced by AES, LEED, and valence states PES data. Subsequent oxygen exposure series left the Si sample surface covered with oxygen. Cleaning of the surface was then achieved simply with a high-temperature anneal (~1000 °C). Thus, the same Si sample was used throughout the whole experiment.

The oxidation procedure used is as follows: (1) Leak in O_2 gas to desired pressure using a variable leak valve and a hot filament ionization gauge; (2) quickly turn on Si sample heater to desired surface temperature; (3) wait for desired exposure time; (4) turn off Si sample heater; (5) quickly close the leak valve and pump away the O_2 gas. Since there is a time constant involved with the O_2 pressure change and the Si substrate temperature change, we use a long exposure time (step 3) in order to neglect the oxygen exposure from the other four steps. Comparing O_2 pressure and exposure time during step 3 with their counterparts from the other four steps, estimated contribution in oxygen exposure [(exposure)=(pressure)×(time)] from steps 1, 2, 4, and 5 is less than 5%. The sample can be raised to the desired temperature within 30 seconds after the heater is turned on and can be cooled down to 200 °C within 15 sec even from 700 °C (the highest oxidation temperature in this experiment), after the heater is turned off. We see that this transient temperature effect on the oxygen uptake data becomes even less significant if we realize that the oxygen uptake rate is diminished at lower temperatures.

III. RESULTS

A. AES measurements of the oxygen coverage

The AES spectra were taken in the first derivative mode, so peak-to-peak heights of the Auger signals were measured. Data was taken for the Si(LVV) Auger signal at 92 eV kinetic energy and the O(KLL) Auger signal at 510 eV kinetic energy. Si(LVV) Auger electrons were used instead of Si(KLL) Auger electrons, because Si(KLL) Auger electrons exhibit strong angular (diffraction) effects.[9] The electron escape depths of Si(LVV) and O(KLL) Auger electrons are 5.5 Å (Ref. 9) and 11 Å (Ref. 14), respectively. Therefore, the $I(\mathrm{O}(KLL))/I(\mathrm{Si}(LVV))$ peak-to-peak height ratio is a good measure of the amount of adsorbed oxygen, if the number of adsorbed oxygen atoms is small and these atoms do not penetrate the Si substrate very deeply (say $d < 5$ Å, which is about the depth of the top four Si layers). For this reason, the $I(\mathrm{O}(KLL))/I(\mathrm{Si}(LVV))$ peak-to-peak height ratio is used throughout this work as a measure of the relative amount of oxygen uptake and will henceforth be referred to as the $I(\mathrm{O})/I(\mathrm{Si})$ ratio. The $I(\mathrm{O})/I(\mathrm{Si})$ ratio is plotted on the (Si substrate temperature)—(O_2 exposure) plane in Fig. 1. The results can be classified into three temperature regions: (1) At room temperature (20 °C) the ratio quickly saturates at 10—30 L and then a slow adsorption step occurs with further exposure; (2) in the medium-temperature range (300—500 °C), no significant difference is observed at low exposures ($< 30L$), while enhancement of oxygen uptake occurs at high exposures, compared with the result at 20 °C; (3) at high temperatures (700 °C and probably above), oxygen adsorption is strongly suppressed at low exposures below 300 L and then rapidly increases at higher exposures. The result at room temperature (20 °C) is in agreement with the previous results,[1–9] although the transition exposure from the fast to the slow adsorption step (10—30 L) is much less than that for unexcited O_2 adsorption (10^3 L) because of hot filament effects on oxidation.[4,9] The fast adsorption step is generally recognized as a simple adsorption of molecular and/or atomic oxygen onto the top Si layer even though other configurations may coexist. On the other hand, the slow adsorption step is involved with a diffusion or

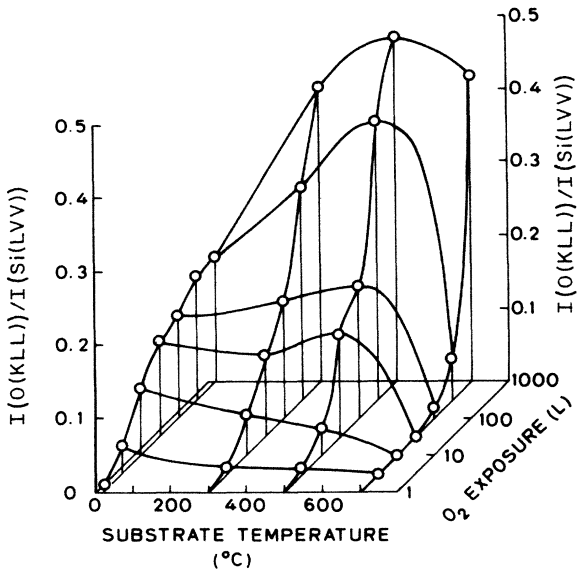

FIG. 1. $I(O(KLL))/I(Si(LVV))$ Auger peak-to-peak height ratio plotted on the (Si substrate temperature)—(O_2 exposure) plane.

penetration of oxygen atoms into the Si substrate, accompanied by bond breaking between Si atoms. The result at 300—500 °C gives us important information on how temperature affects the fast and slow adsorption steps. The fast adsorption step is almost independent of temperature, while the slow adsorption step is enhanced with increasing temperature probably because thermally-induced atomic vibration allows for easier penetration of the oxygen atoms. The oxidation behavior at 700 °C is quite different from the lower-temperature results. Strong suppression of oxygen uptake can be explained by the formation of volatile SiO molecules.[15,16] SiO, rather than SiO_2, is the thermodynamically stable form of silicon oxide under certain oxidation conditions. According to Gelain *et al.*,[16] at 700 °C a thin film of SiO_2 is formed ("passivation" mode of oxidation) only when the O_2 pressure is greater than $\sim 3\times 10^{-7}$ Torr. For O_2 pressure below $\sim 3\times 10^{-7}$ Torr, volatile SiO is formed ("combustion" mode of oxidation), and the Si surface is being etched away by oxygen atoms. The transition between these two modes of oxidation is quite abrupt, and there is a transition pressure associated with each temperature. This transition pressure increases with increasing temperature. Therefore, O_2 pressure, rather than O_2 exposure [(exposure)=(pressure)×(time)], is the important parameter to consider when SiO formation is significant. Pressures used for all exposures are listed in Table I. Extrapolating from the results of Gelain *et al.*,[16] all the exposure conditions at 500 °C and below should produce oxidation in the passivation mode. For 700 °C all the exposure conditions above 100 L should also produce oxidation in the passivation mode, while those below 100 L oxidation in the combustion mode. The AES results in Fig. 1 are in good agreement with this model of oxidation.

B. Relation between LEED patterns and surface states

Basically, three types of LEED results were observed: i.e., 7×7, 1×1, and no pattern. It is well known that a clean annealed Si (111) surface yields a 7×7 LEED pattern. Since we heat clean the Si sample, this is always the pattern we start with. As O_2 exposure increases, the pattern changes into a 1×1 pattern. With further exposure, the 1×1 pattern disappears into no pattern. The results are summarized in Fig. 2. Since the 7×7 spots slowly fade into 1×1 spots and similarly the 1×1 spots gradually disappear, these transitions are not sharp and are somewhat subjectively determined. The 7×7, mixture of 1×1 and weak 7×7, 1×1, weak 1×1, and no pattern are marked A, A′, B, B′, and C, respectively. From Fig. 2 it can be seen that the 1×1 pattern region occurs at almost the same O_2 exposure ($\sim$10 L) at $T \leq 500$°C and at a much higher exposure ($\sim$300 L) for $T = 700$ °C. By referring back to Fig. 1 we see that all the points in the 1×1 pattern region seem to have about the same $I(O)/I(Si)$ ratio. Therefore, the 1×1 LEED pattern is produced by the same amount of adsorbed oxygen for all temperatures. In other words, the LEED pattern transition seems to be governed only by the amount of adsorbed oxygen, although the amount of adsorbed oxygen is

TABLE I. (a) O_2 pressures used for exposures (1 L = 1 langmuir = 10^{-6} Torr sec). (b) Transition O_2 pressure between passivation and combustion mode of oxidation for different Si substrate temperatures (after Ref. 16).

(a)

O_2 exposure (L)	O_2 pressure (Torr)
3	1×10^{-8}
10	3.5×10^{-8}
30	1×10^{-7}
100	3.5×10^{-7}
300	1×10^{-6}
1000	3.5×10^{-6}

(b)

Si substrate temperature (°C)	O_2 pressure (Torr)
900	1×10^{-4}
700	3×10^{-7} (extrapolated)
500	1×10^{-11} (extrapolated)

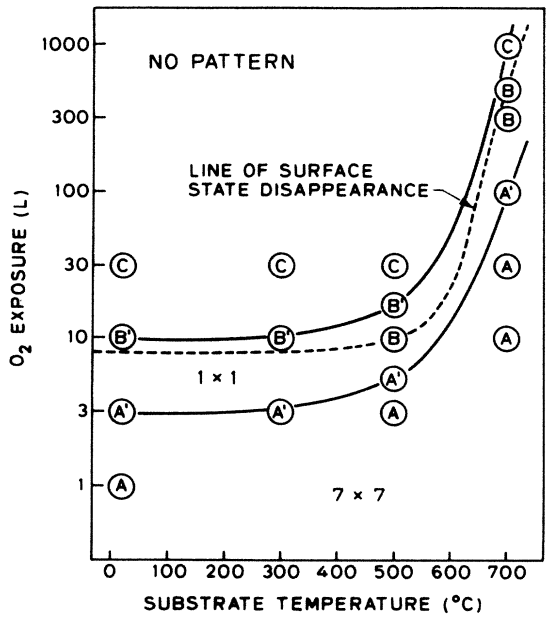

FIG. 2. LEED pattern map plotted on the (Si substrate temperature)—(O_2 exposure) plane.

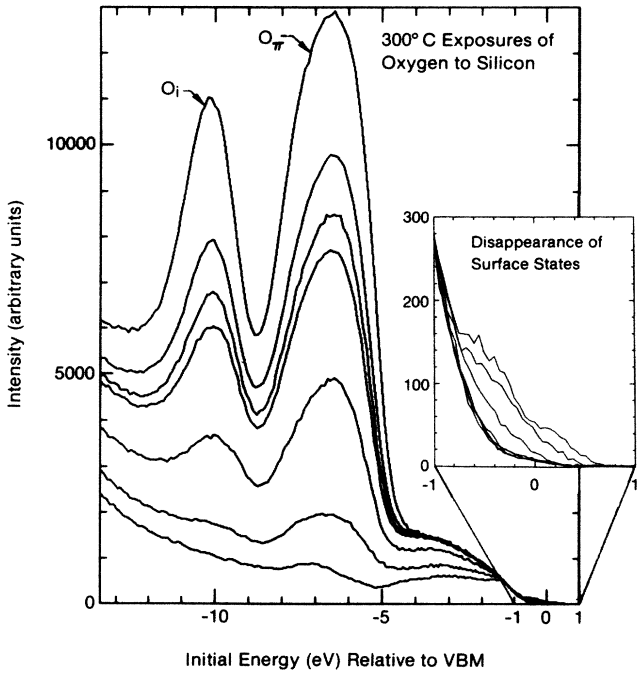

FIG. 3. Typical series of valence states PES data for increasing O_2 exposures, obtained using monochromatized He I (21.2 eV) light. Band bending effects have been removed, so we can plot the initial energy of photoelectron relative to the bulk Si valence-band maximum (VBM). The spectrum of lowest intensity is from the clean Si(111)-(7×7) surface. Following that, the intensity of the spectrum increases with increasing O_2 exposures, which were 3, 10, 30, 100, 300, and 1000 L. Inset shows a blow-up of the region around VBM, allowing one to better see the disappearance of surface states centered about 0.6 eV below the VBM. The series shown is for 300 °C exposure temperature.

dependent on temperature. The transition exposure ($\sim$10 L) between the fast and slow adsorption steps at 20 °C also lies in this 1×1 pattern region, so it is possible that the 1×1 LEED pattern is caused by relaxation of the 7×7 surface through molecular or atomic oxygen adsorption to surface Si dangling bonds.[9] We have found, however, that this interpretation is too straightforward, as will be described in Section IV.

A typical series of valence states PES data for increasing O_2 exposure is shown in Fig. 3, where the incident photon energy is 21.2 eV (He I). Peaks (which originate from the O 2*p* orbital) at 7 eV and 10.7 eV below the valence band maximum (VBM) will be discussed later. Here, let us pay attention to the surface state peak at 0.6 eV below the VBM. The surface state peak is due to photoelectron emission from electronic states associated with the surface Si atoms.[17] Wagner and Spicer[17] reported the location of the surface state peak to be 1.1 eV below the surface Fermi level or 0.6 eV below the VBM. (The surface states do not appear as a well-resolved peak, but their presence as a protruding shoulder is clearly seen in our data.) Because surface states are associated with surface atoms or probably surface dangling bonds, it is anticipated that adsorbed oxygen will remove them, as reported by Wagner and Spicer[17] and as shown in the inset of Fig. 3. The exposure values at which the surface states disappear are plotted in Fig. 2. It is seen that the curve lies in the 1×1 LEED pattern region or in the 1×1 to the no pattern transition region. The reported exposure for the disappearance of surface states was $\sim 10^3$ L at room temperature,[9,17] while 10 L was found in this work. We confirmed that this discrepancy was caused by the presence of a hot filament ion gauge in our work, by repeating the experiment with a cold cathode gauge. The repeated experiment resulted in the same exposure as previous works.[9,17]

Thus, the results are summarized as follows: (1) The 1×1 LEED pattern is produced by the same amount of adsorbed oxygen, regardless of exposure temperature; (2) this amount of adsorbed oxygen is equal to that found for the transition exposure between the fast and slow adsorption steps at 20 °C; (3) the surface states (centered about 0.6 eV below the VBM) disappear at the same O_2 exposure that produces the 1×1 LEED pattern, so their disappearance also seems to be brought on by this same amount of adsorbed oxygen.

C. The Si 2*p* core level

PES data of the Si 2*p* core level was taken at $h\nu = 130$ eV in order to examine the microscopic atomic bonding and chemical nature of the surface oxidized layer. The incident photon energy, 130 eV, was chosen because it excited the most surface sensitive photoelectrons [electron escape depth of 4.5 Å (Ref. 9)] from the Si 2*p* core level and because the SSRL 4° line monochromator gave the highest photon flux at this photon energy. The incident photon flux changes during the entire course of the experiment because we use synchrotron radiation from an electron storage ring and the stored electron beam slowly decays with time. Therefore, we had to normalize out the photon flux changes. Figure 4 shows a series of normalized PES

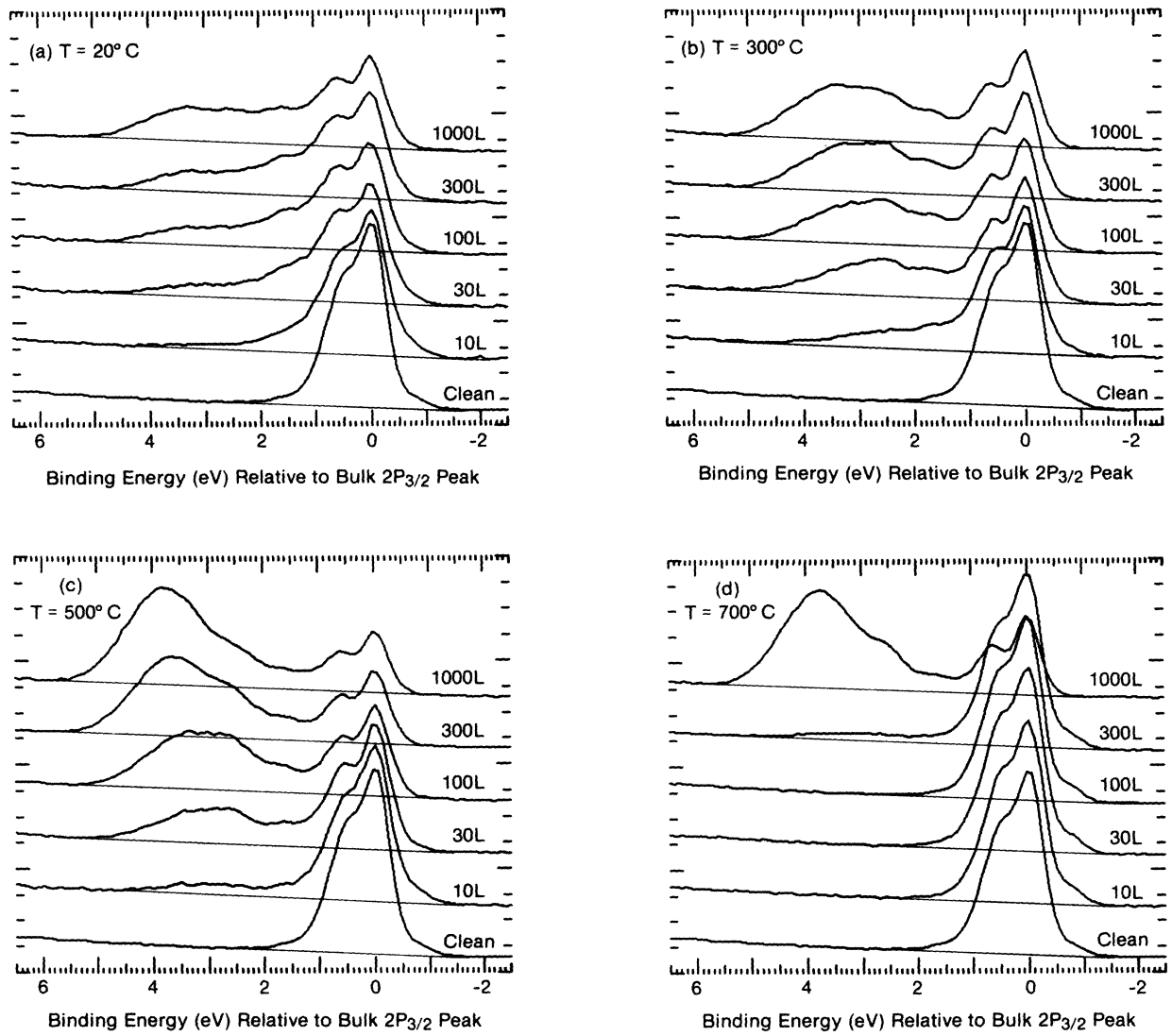

FIG. 4. PES data of Si $2p$ core level taken at $h\nu = 130$ eV for increasing O_2 exposures. The O_2 exposures are expressed in units of langmuir (1 langmuir $= 1$ L $= 10^6$ Torr sec). The Si substrate temperatures were (a) 20 °C (room temperature), (b) 300 °C, (c) 500 °C, and (d) 700 °C. The spectra have been normalized with respect to variations in incident photon flux. Energy shifts of the bulk Si $2p_{3/2}$ peak due to band bending have also been removed.

spectra taken at four different exposure temperatures.

For the clean surface a shoulder is observed on the low-binding-energy side of the spin-orbit split Si $2p_{1/2,3/2}$ doublet, and the doublet is not well resolved as separated peaks because surface-shifted components are superimposed onto the bulk doublet.[18,19] O_2 exposure of the clean surface, however, quenches this surface contribution so that the shoulder disappears and clearly separated peaks (0.6 eV splitting) of the bulk doublet are observed. Furthermore, O_2 exposure introduces chemically shifted core levels on the high-binding-energy side of the bulk peak. For the study of the chemically shifted core levels, we first perform background subtraction on both the clean and oxidized spectra. Then we subtract the clean spectrum from the oxidized spectrum after adjusting the height of the bulk Si $2p_{3/2}$ peak in the clean spectrum to that of the unshifted Si $2p_{3/2}$ peak in the oxidized spectrum. The results are shown in Fig. 5. Elimination of the unshifted Si $2p$ core level is not perfect, and we see wiggles at the unshifted Si $2p$ core-level position in Fig. 5, because the clean spectrum includes contributions from the surface-shifted peaks. The difference curves are, however, both helpful and satisfactory for the discussion of oxygen-induced chemically shifted levels.

In Fig. 4 and more clearly in Fig. 5, four distinct peaks are observed with shifted energies of 1.0, 1.7, 2.6, and ~ 3.6 eV toward higher binding energy relative to the bulk Si $2p_{3/2}$ peak. This is most obvious in the 1000 L difference spectrum of Fig. 5(d). They belong to the incompletely oxidized Si atoms found by Garner *et al.* (1.0, 2.0, 2.9, and 3.8 eV) (Ref. 9), Grunthaner *et al.* (1.1, 2.1, 3.1, and 4.3 eV) (Refs. 20 and 21), and Hollinger and Himpsel (1.0, 1.8, 2.7, and 3.5 eV) (Refs. 22–24). Our values are very close to those of Hollinger and Himpsel.[22–24] Attempting to understand the physical basis for these chemical shifts, we have attributed them to differing numbers

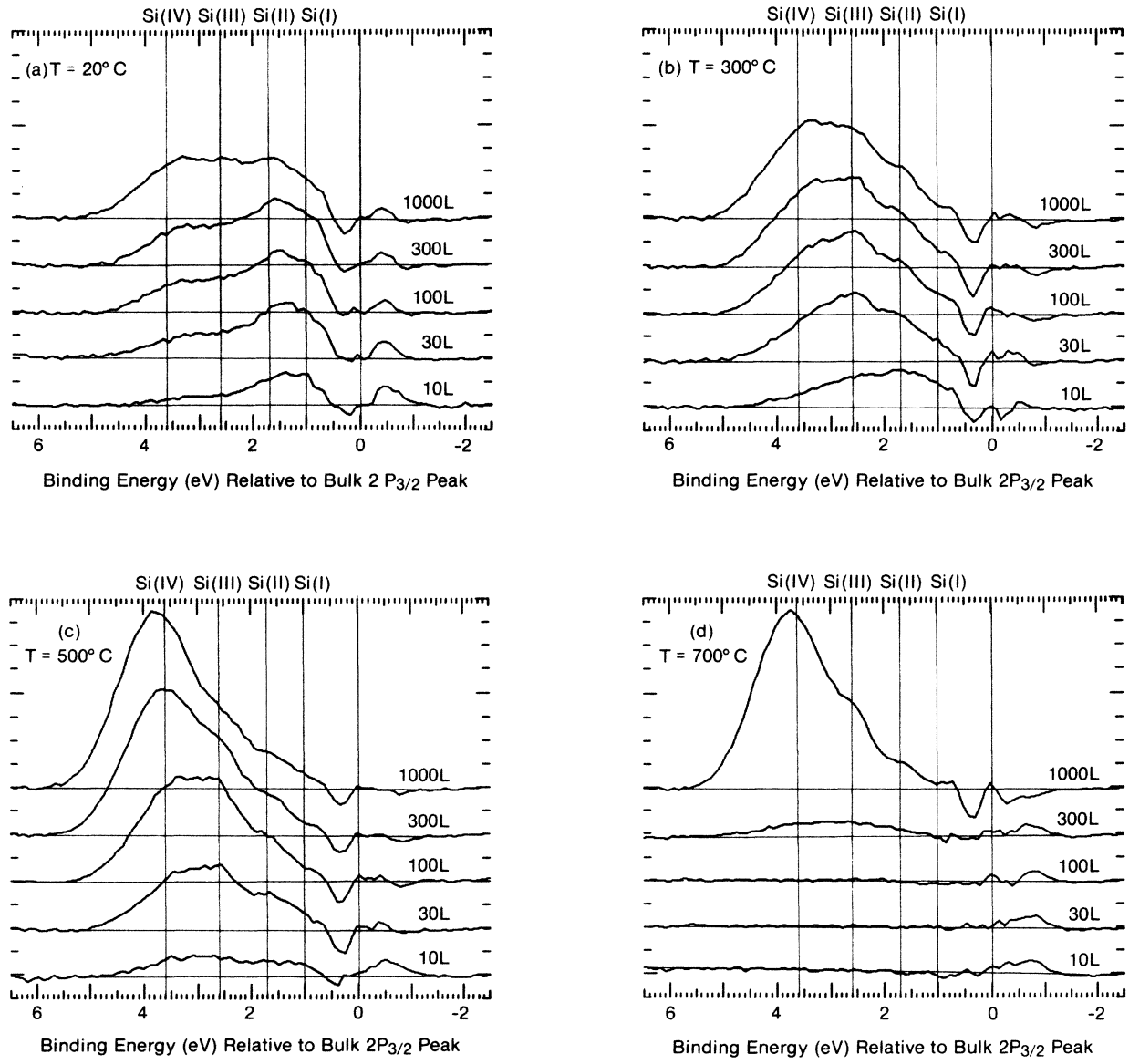

FIG. 5. Si $2p$ difference spectra (obtained from Fig. 4). The unshifted Si $2p_{3/2,1/2}$ peaks have been subtracted away, so one can view the chemically shifted peaks more clearly. (See Sec. III C for details of the subtraction procedure. The wiggles at the unshifted Si $2p$ core-level position are due to surface-shifted peaks present in the clean spectrum used for subtraction.) The Si substrate temperatures were (a) 20 °C (room temperature), (b) 300 °C, (c) 500 °C, and (d) 700 °C. The Si(I) chemically shifted peak is due to Si atoms with one oxygen atom bonded to each Si atom. The Si(II) peak is due to Si atoms with two oxygen atoms bonded to each Si atom and so on.

of oxygen atoms attached to each Si atom following the work by Hollinger and Himpsel.[23] The notation we use is Si(I) for a Si atom with one oxygen atom bonded to it, Si(II) for a Si atom with two oxygen atoms bonded to it, and so on. The energy positions of Si(I), Si(II), and Si(III) are unchanged, whereas the position of Si(IV) seems to vary from 3.5 to 3.9 eV with oxidation [see a series of 500 °C exposures in Fig. 5(c)]. This shifted energy change in Si(IV) is possibly due to an increase in the bridging oxygen bond angle θ from a low value ($\sim 100°$) to 144°, which is the value for α quartz.[10,20] This may be viewed as a form of strain relaxation.

The peak heights of Si(I), Si(II), Si(III), and Si(IV) were directly plotted in Fig. 6 as a function of the amount of oxygen uptake [$I(\mathrm{O}(KLL))/I(\mathrm{Si}(LVV))$ ratio]. Choosing the oxygen uptake amount as the abscissa allowed us to observe the chemical bonding dependence on temperature and eliminate the oxygen uptake rate dependence on temperature. If O_2 exposure was selected as the abscissa, the oxygen uptake rate dependence on temperature would have also been included, complicating the data analysis. For example, if we found 500 °C to have a larger Si(III) peak than 20 °C at 30 L O_2 exposure, is this increase simply due to an enhanced oxygen uptake rate at 500 °C or is this increase due to a fundamentally different form of oxide [i.e., one which possesses a higher fraction of Si(III) atoms] being formed at 500 °C?

Looking at Fig. 6 it is obvious that (1) the Si(I) and

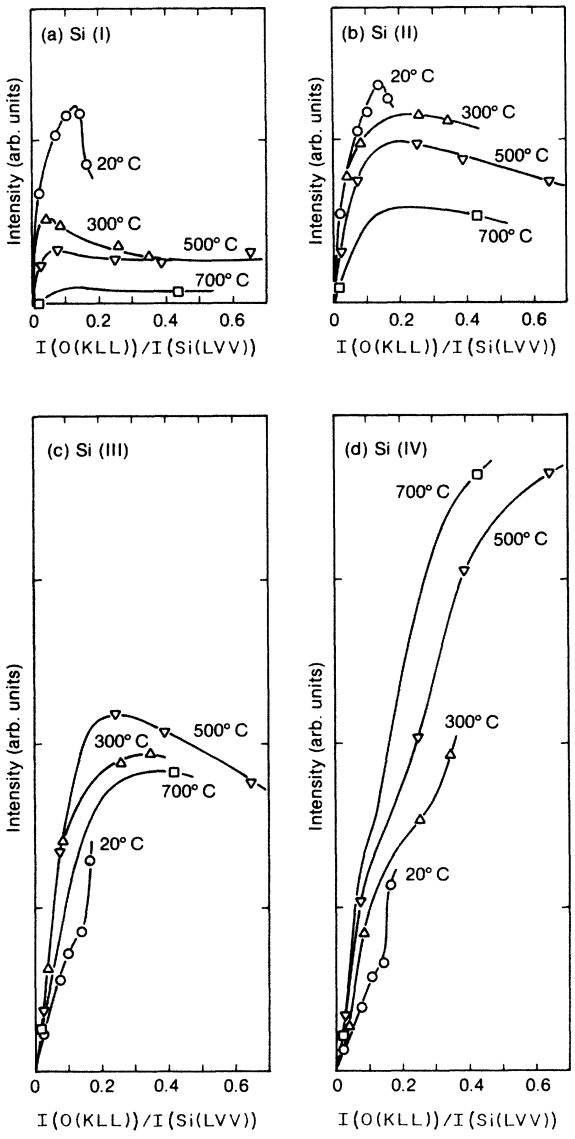

FIG. 6. Peak heights of chemically shifted components (obtained from Fig. 5) plotted as a function of the amount of oxygen uptake [I(O(KLL))/I(Si(LVV)) Auger peak-to-peak height ratio]. (a) was for the Si(I) chemically shifted peak, (b) for Si(II), (c) for Si(III), and (d) for Si(IV).

Si(II) intensities become smaller with increasing temperature at any I(O)/I(Si) ratio; (2) the Si(III) and Si(IV) intensities become higher with increasing temperature except for a few data points; (3) Si(I), Si(II), and Si(III) have maximum intensities, whereas Si(IV) increases monotonically with increasing I(O)/I(Si) ratio. Points (1) and (2) suggest that at elevated temperatures oxidation proceeds in a nonuniform or phase-separated fashion, while at room temperature oxidation proceeds more uniformly. To understand this, we first notice that the abscissa of Fig. 6 is the I(O)/I(Si) ratio, so we are comparing the data for a fixed number of oxygen atoms. For the higher-temperature-grown oxides, there is a higher fraction of Si(III) and Si(IV) atoms, so the oxidized silicon atoms have a larger number of oxygen atoms per silicon atom. This means that the oxygen atoms are bonding to fewer silicon atoms, but these silicon atoms have more oxygen atoms bonded to them and are hence closer to the SiO_2 configuration. The crude picture (i.e., not totally correct, but helping one get a feel for what is going on) one can draw from this is little pockets of SiO_2-like material distributed in the Si substrate (phase-separated fashion of oxidation). For the room-temperature-grown oxide, there is a higher fraction of Si(I) and Si(II) atoms, so the oxidized silicon atoms have a smaller number of oxygen atoms per silicon atom. This means that the oxygen atoms are bonding to more silicon atoms, but these silicon atoms have fewer oxygen atoms bonded to them. The crude picture one can draw from this is a uniform distribution of oxygen atoms in the Si substrate (uniform fashion of oxidation). Heating the Si substrate allows the oxygen atoms to phase separate into the thermodynamically favored SiO_2 configuration, while lowering the substrate temperature forces the oxygen atoms to go on more uniformly.

Looking at this from another point of view, we first consider oxidation occurring in a layer-by-layer (uniform) manner: The first oxidation step will be oxygen adsorption onto the topmost Si layer [see Fig. 7(a) for actual

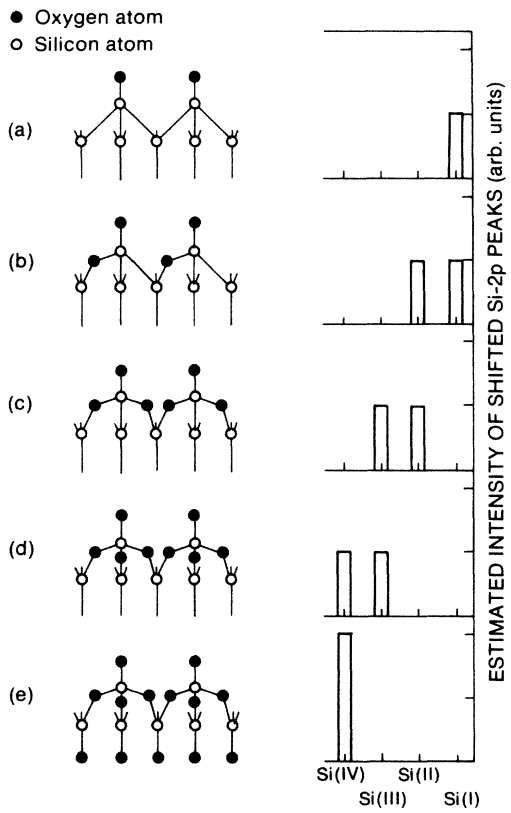

FIG. 7. Possible atomic bonding geometries useful for considering the initial stage of oxidation of the Si(111) surface. These atomic bonding geometries simulate the process of oxygen incorporation into the Si lattice, if oxidation occurs in a uniform, layer-by-layer fashion. The estimated intensities of the various chemically shifted Si $2p$ peaks are shown to the right of the bonding geometry they represent. Assumptions used for estimating the intensities are discussed in Sec. IV A, but basically the top two Si layers contribute equally to the peak intensities while contributions from deeper layers are ignored.

atomic arrangement]; when all the topmost adsorption sites are filled, the second step will occur, and it is the penetration of oxygen atoms into the bridge sites between the first and second Si layers [see Fig. 7(d)]; after all the bridge sites are filled, the third step will occur, and it is the penetration of oxygen atoms into the bridge sites between the second and third Si layers [see Fig. 7(e)] and so on. In the first step Si(I) species will be expected to dominate. Then, with increasing oxygen uptake, Si(II), Si(III), and Si(IV) species will successively dominate. When we look at the early stages of oxidation [$I(O)/I(Si) < 0.1$], the result at 20 °C [see Fig. 5(a)] seems to follow this tendency. The results at elevated temperature, however, look different [e.g., at 300 and 500 °C, Si(III) rather than Si(I) is dominant at $I(O)/I(Si) < 0.1$]. Therefore, at elevated temperatures, the oxygen atoms appear to have penetrated more deeply and the Si atoms more fully oxidized (i.e., getting closer to the SiO_2 configuration). However, we are comparing the results at the same $I(O)/I(Si)$ ratio, so the oxidation at elevated temperature must deviate from the layer-by-layer (uniform) fashion and must occur in a nonuniform, phase-separated fashion (i.e., some areas getting oxidized faster than other areas). More detailed analysis will be described in Sec. IV.

Finally, in both layer-by-layer (uniform) and nonuniform oxidation, the final product is Si(IV) atoms (i.e., Si in SiO_2 configuration), so the Si(IV) peak should increase monotonically with increasing oxygen coverage. However, to obtain Si(IV) atoms, one needs to go through Si(I), Si(II), and Si(III) states as these are the incompletely oxidized Si states. We expect to see these states at all oxygen coverages but do not expect their intensities to exceed a maximum value, as Si(IV) is the thermodynamically preferred state and these are just Si atoms on their way to becoming Si(IV) atoms. We notice this consideration is quite consistent with the observation of point (3), i.e., the population of Si atoms bonded to four oxygen atoms increases monotonically, while the population of Si atoms bonded to less than four oxygen atoms peaks and then decreases with increasing oxygen exposure.

D. The O-2p peaks in valence states PES data

Two prominent peaks relevant to oxidation were observed in the PES data in the vicinity of the valence band as shown in Fig. 3. Their energy positions are 7.0 and 10.7 eV below the VBM. According to a tight-binding calculation of β-cristobalite (SiO_2) reported by Pantelides and Harrison,[25] in the valence band there are two sets of bands relevant to O 2p. The lower binding-energy band originates from nonbonding O 2p orbitals oriented normal to the bonding direction, whereas the higher binding energy originates from bonding O 2p orbitals which interact with neighboring Si $3sp^3$ orbitals. The location of each band is 0—3 eV and 5—11.5 eV, respectively, below the valence band maximum (VBM) of β-cristobalite (SiO_2). This approximates to 4.5—7.5 eV and 9.5—16 eV below the VBM of Si, assuming the VBM of β-cristobalite (SiO_2) is 4.5 eV below the VBM of Si.[17] Thus, it seems reasonable to attribute the two observed peaks to nonbonding and σ-bonding O 2p orbitals, since each theoretical energy range covers the location of the observed peak.

Ciraci *et al.*[26] have calculated density of states for the oxygen-adsorbed and oxidized silicon surfaces using an empirical tight-binding method. According to their result, the lower binding-energy peak (O π) at 12.4 eV below the vacuum level (or 7.0 eV below the VBM, if we assume $E_{VL} - E_{VBM} = 5.4$ eV, where VL stands for vacuum level; Ciraci *et al.* had adjusted the self-energies of O s and p orbitals such that the peak produced by the O 2p nonbonding orbitals coincides with the dominant PES peak) has nonbonding or π-bonding O 2p character while the higher binding-energy peaks (O σ) at 18.4 and 19.6 eV below the vacuum level (or 13.0 and 14.2 eV below the VBM) have more or less σ-bonding O 2p character. These states are seen when we have atomic oxygen chemisorbed on the topmost layer of the Si(111) surface [i.e., fast adsorption step; see Fig. 7(a) for actual atomic arrangement]. An additional peak at 14.8 eV below the vacuum level (or 9.4 eV below the VBM) is observed when the oxygen atoms have penetrated into the bridge sites between the topmost and second topmost Si layers [i.e., slow adsorption step; see Fig. 7(b) for actual atomic arrangement]. This additional peak is called O i because it has an intermediate character between nonbonding and σ-bonding O 2p orbitals.

The present and previous experimental results of peak positions are summarized in Fig. 8 together with theoretical results. The results of Pantelides and Harrison are shown in 8(e) (Ref. 25), while the results of Ciraci *et al.* are shown in 8(f) (Ref. 26). The present work's experimental results are shown in 8(a). Looking at Fig. 8 it is easy to assign the experimental peak at -7 eV (relative to the VBM) as the O π peak. It is less easy to make the assignment for the experimental peak at -10.7 eV, since it lies between the theoretical peaks O i (-9.4 eV) and O σ (-13.0 eV). Nevertheless, O i is still probably the right assignment because the O i peak should be the first peak immediately following the O π peak. Therefore, we name

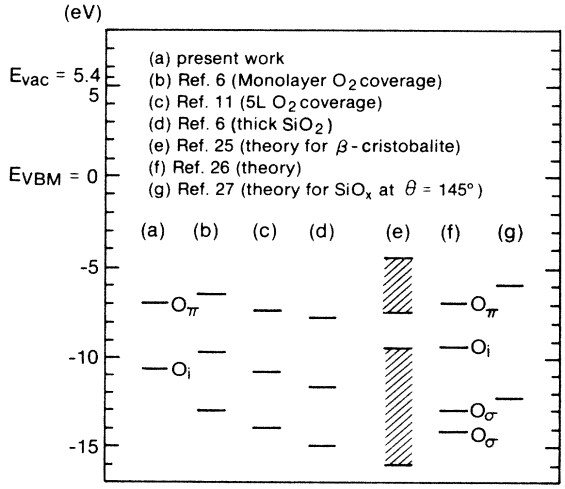

FIG. 8. Summary of valence state peak positions obtained from various experimental and theoretical works. The O σ peak was absent in our data (a), probably because the secondary electron tail obscured it.

the experimental peaks at -7 eV and -10.7 eV O π and O i, respectively, and these are their labels in Fig. 8. The O σ peak was absent in our data because 21.2 eV (He I) light was used. The O σ peak was probably obscured by the huge secondary electron tail. With 40.8 eV (He II) light, we probably would be able to see the O σ peak.

Figure 9 shows the peak height ratio of O i to O π at different temperatures as a function of oxygen uptake. Since the height of O π is almost proportional to the $I(\mathrm{O}(KLL))/I(\mathrm{Si}(LVV))$ ratio and independent of the oxidation temperature (figure not shown), each curve reflects the behavior of O i. To understand the origins of the O i states, we recall that they appear when oxygen atoms are inserted into bridge sites between the topmost and second topmost Si layers. Therefore, it is reasonable to assume the O i states result from the Si—O—Si bridge bond. Ciraci *et al.* checked this assumption by performing calculations on a few Si-O systems and concluded that indeed the O i states resulted from the Si—O—Si bridge bond.[26] Armed with this knowledge, we expect the $I(\mathrm{O}i)/I(\mathrm{O}\pi)$ ratio to be a qualitative measure of the number of bridge-site oxygen atoms. Applying this interpretation to Fig. 9, it is seen that higher temperature gives rise to a larger number of bridge-site oxygen atoms [higher values of the $I(\mathrm{O}i)/I(\mathrm{O}\pi)$ ratio] even at the same amount of oxygen uptake. This means that at elevated temperatures more oxygen atoms are penetrating below the top Si layer, and, referring back to the Si $2p$ core-level analysis, we would infer that oxidation occurs in a nonuniform or phase-separated fashion. Once again, the result supports a nonuniform phase-separated type of oxidation. However, a quantitative relation between the $I(\mathrm{O}i)/I(\mathrm{O}\pi)$ ratio and the number of bridge-site oxygen atoms has not been established, so this interpretation is somewhat speculative. A similar interpretation, however, can be derived from a different viewpoint. Lannoo and Allan reported the valence density of states of bulk amorphous SiO_x using a tight-binding treatment.[27] Looking at Figure 5 of Lannoo and Allan's paper,[27] we observe a -6-eV (relative to the VBM) and a -12.3-eV peak. These peaks are shown in Fig. 8(g). We make the assignments of O π and O i for the -6-eV and -12.3-eV peaks, respectively. In Fig. 10 the $I(\mathrm{O}i)/I(\mathrm{O}\pi)$ peak height ratio (from the calculations of Lannoo and Allan) is plotted versus x in SiO_x. Lannoo and Allan calculated the density of states for different x values with the Si—O—Si bond angle fixed at 145° and only for $x=\frac{4}{3}$ with the angle fixed at 120° and 100°. Therefore, only the results of 145° are available for plotting in Fig. 10. From Fig. 10 it is seen that the $I(\mathrm{O}i)/I(\mathrm{O}\pi)$ ratio increases monotonically with increasing x value. Looking at Fig. 9 and staying at a fixed $I(\mathrm{O})/I(\mathrm{Si})$ ratio, we notice the higher-temperature-grown oxide has a higher $I(\mathrm{O}i)/I(\mathrm{O}\pi)$ ratio than the lower-temperature-grown oxide. Referring to Fig. 10 this means the higher-temperature-grown oxide has a higher value of x than the lower-temperature-grown oxide, if we assume these small islands of surface oxide to behave like bulk amorphous SiO_x. In other words, the higher-temperature-grown oxides are more completely oxidized and, since we are comparing at fixed $I(\mathrm{O})/I(\mathrm{Si})$ ratio, we are once again led to conclude that nonuniform or phase-separated type of oxidation occurs at high temperature. In summary, the nonuniform or phase-separated type of oxidation at elevated temperature, suggested by the Si $2p$ core-level analysis, is con-

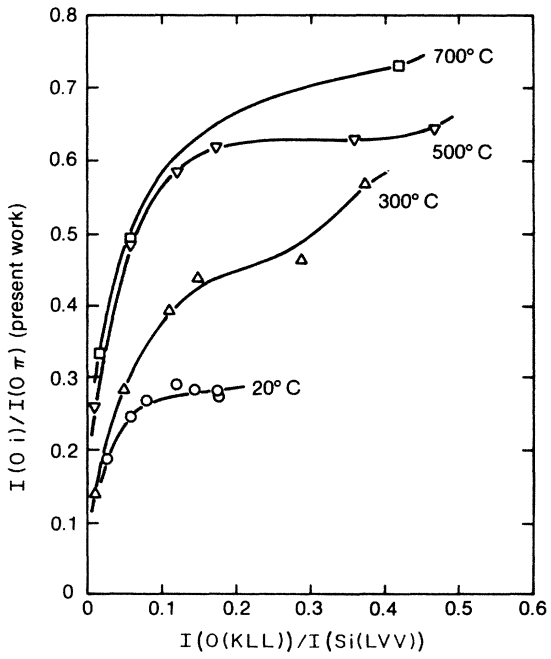

FIG. 9. Experimental $I(\mathrm{O}i)/I(\mathrm{O}\pi)$ peak height ratio plotted as a function of the amount of oxygen uptake [$I(\mathrm{O}(KLL))/I(\mathrm{Si}(LVV))$ Auger peak-to-peak height ratio].

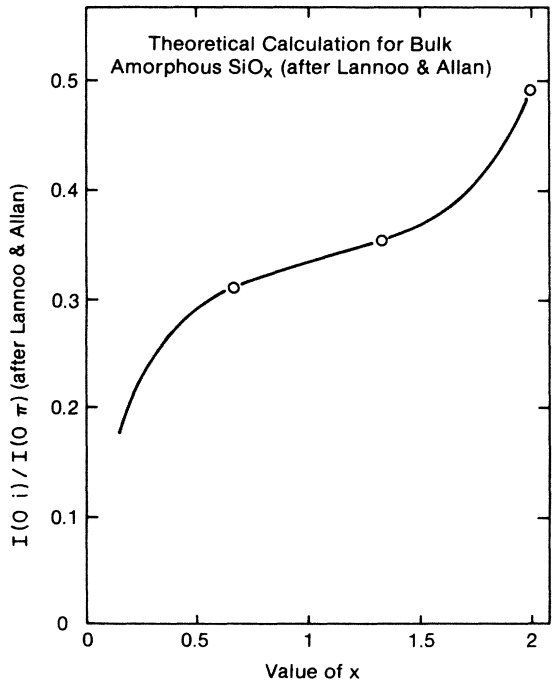

FIG. 10. Theoretical $I(\mathrm{O}i)/I(\mathrm{O}\pi)$ peak height ratio plotted as a function of x. The O i and O π peak heights were obtained from theoretical calculations for bulk amorphous SiO_x performed by Lannoo and Allan (Ref. 27). The calculations assumed the Si—O—Si bond angle was 145°.

firmed through qualitative analysis of the $I(O\,i)/I(O\,\pi)$ peak height ratio obtained from valence states PES data.

IV. DISCUSSION

A. Atomic bonding geometries for the oxidized surface

Our experimental results strongly suggest at elevated temperatures oxidation proceeds in a nonuniform or phase-separated fashion. Attempting to understand how this occurs on the atomic bonding level, we propose some possible bonding geometries in Fig. 7, together with the estimated intensities of the various chemically shifted Si $2p$ peaks. For simplicity, the following assumptions are used in making our estimations:

(1) The signal height at each shifted peak is proportional to the number of Si atoms bonded by the specific number of oxygen atoms [e.g., Si(I) is bonded by one oxygen atom, Si(II) by two oxygen atoms, etc.].

(2) The first and second Si layers contribute equally to the signal intensities and only these two layers are taken into account. Contributions from the third and deeper layers are completely ignored. (According to a simple calculation using the electron escape depth of 4.5 Å, contributions from the first, second, and third layers are reduced by a factor of 1, 0.77, and 0.465, respectively, ignoring the effect of oxygen atoms on the Si lattice spacing.)

The proposed bonding geometries are definitely not meant to illustrate exactly what happens on the atomic level, because the actual situation is very complicated. Even the atomic arrangement of the clean Si(111)-(7×7) reconstructed surface is not very well known and you will notice that in Fig. 7, instead of making wild guesses at the actual atomic arrangement of the 7×7 reconstructed surface, we have simply assumed 1×1 bulklike periodicity for the clean Si(111) surface.

Looking at Fig. 7 one can clearly see the proposed relation between bonding geometries and shifted peak intensities. In geometry (a) each of the top layer Si atoms have an oxygen atom bonded to it in the top site, while all the second layer Si atoms have no oxygen atoms bonded to it. We will only see the Si(I) peak. In geometry (b) the oxygen atoms have started to penetrate to the bridge sites between the first and second Si layers and, of the three bridge sites connected to each top layer Si atom, only one is occupied. Each of the top layer Si atoms has two oxygen atoms bonded to it, and each of the second layer Si atoms has one oxygen atom bonded to it. Therefore, Si(I) and Si(II) have the same intensities under the assumptions described above. In geometry (c) two of the three bridge sites connected to the top layer Si atom are occupied, so each of the top layer Si atoms has three oxygen atoms bonded to it and each of the second layer Si atoms has two oxygen atoms bonded to it. Now Si(II) and Si(III) have the same intensities. In geometry (d) all the bridge sites between the first and second layer Si atoms are occupied, and we predict Si(III) and Si(IV) to have the same intensities. The top Si layer is completely oxidized [in Si(IV) state], while the second Si layer is still incompletely oxidized [in Si(III) state]. In geometry (e) the oxygen atoms have penetrated to the bridge sites between the second and third Si layers, and have completely occupied the single bridge site available. Both the first and second Si layers are completely oxidized [in Si(IV) state]. Although the third layer Si atom has one oxygen atom bonded to it, we have not shown its contribution to the Si(I) peak intensity, because our assumptions ignore contributions from beyond the second layer. In terms of the total number of oxygen atoms engaged in bonding geometry, geometry (a) has x number of oxygen atoms (x equals the number of top layer Si atoms), geometry (b) has $2x$ number of oxygen atoms, (c) $3x$, (d) $4x$, and (e) $5x$.

Comparing Figs. 5 and 7 we see that none of the Si $2p$ difference spectra can be adequately described by a single bonding geometry. This is not surprising, since the experimental results suggest a nonuniform or phase-separated fashion of oxidation. The actual oxidized surface is expected to consist of a distribution of different bonding geometries, so the Si $2p$ difference spectra of Fig. 5 should be a linear sum of the predicted spectra for these bonding geometries as shown in Fig. 7. Furthermore, we should be able to identify a dominant bonding geometry for each oxygen exposure. The results are summarized in Table II. Significant points derived from Table II are as follows:

(1) Oxidation starts with geometry (b) at 20—300 °C and (d) at 500—700 °C. Geometry (a) or close variations of it (not shown; examples include molecular oxygen adsorption onto the top Si layer) which has been thought to be dominant in the fast adsorption stage at room temperature,[2,5,7,9] is not even found at the lowest oxygen uptake.

(2) At a fixed oxygen uptake level, geometries (b) and (d) are followed by (d) and (e), respectively, with increasing temperature. This tendency has already been described in Sec. III C looking at only Fig. 6.

(3) Penetration of oxygen atoms into the bridge sites between the second and third Si layers, i.e., complete oxidation of the first and second layers, occurs only at 500—700 °C for the oxygen exposures used here.

Difference in dominant geometries at a certain oxygen uptake means difference in the uniformity of oxidation. For example, dominant geometries are (b) for 20 °C and (d) for 300 °C at $I(O)/I(Si)=0.08$—0.10. In order to keep the same $I(O)/I(Si)$ ratio for both surfaces, geometry (b) at 20 °C should be more uniformly distributed over the surface than geometry (d) at 300 °C. Again this point has already been described in Sec. III C looking at only Fig. 6.

In summary, we conclude that high-temperature oxida-

TABLE II. List of dominant bonding geometries at various amounts of oxygen uptake and differing Si substrate temperatures. Notation in the table follows the definition given in Fig. 7.

T (°C) / $I(O)/I(Si)$	20	300	500	700
0.02—0.04	(b)	(b)	(d)	(d)
0.08—0.10	(b)	(d)	(d)	
0.20—0.25	(d)	(d)	(d)	
0.40—0.44		(d)	(e)	(e)

tion causes nonuniform growth of oxide in the early stage before the first three Si layers are completely oxidized. According to previous results on the question of abruptness of SiO_2-Si interface,[9,24,28,29] the thickness of 5 Å or less is generally accepted for the transition region. Assuming this abruptness is maintained even by the very thin oxide films studied in this work, it is suggested that geometries from (a) to (e) can coexist on the surface, since the thickness of 5 Å includes nearly two or three Si layers. Coexistence of other geometries whose oxidized depth is deeper than (e) is unlikely because they will create a transition region thicker than 5 Å. Consequently, it is anticipated that, in the oxidation steps beyond Table II, the corresponding bonding geometries should conserve the same transition region thickness. An obvious way for this to occur is to continue adding oxygen atoms into the bridge sites between successive Si layers. The transition region for this bonding geometry will be at most 2.34 Å thick (i.e., maximum distance between two successive Si layers in the ⟨111⟩ direction). Although our study seems to suggest that lower-temperature oxidation leads to a more abrupt interface because it proceeds in a more uniform fashion, further study is necessary to discuss the temperature dependence of abruptness in a quantitative manner.

B. LEED and the disappearance of surface states

The experimental result described in Sec. III B indicates that the pattern change of LEED and the disappearance of surface states seem to be governed only by the amount of oxygen uptake. The exposure temperature seems to have no significant effect except through variation of the amount of oxygen uptake. Dominant geometries in the 1×1 pattern region and at the disappearance of surface states are (b) for 20 °C, (b)—(d) for 300 °C and (d) for 500 and 700 °C. Since these geometries are quite different from (a) and close variations of it (e.g., molecular oxygen adsorption onto the top Si layer), the 1×1 pattern and the disappearance of surface states cannot be straightforwardly attributed to the termination of surface dangling bonds by atomic or molecular oxygen. However, if geometry (b) is locally achieved as in the case of 20 °C, the less-oxidized surface or clean surface around this geometry may rearrange itself to relax the strain and lower its energy. This could result in the 1×1 LEED pattern as well as the disappearance of surface states. Similarly, if geometry (d) is locally formed as in the case of 700 °C, a larger rearrangement would be expected because of the bigger strain around geometry (d) than geometry (b). Therefore, although the total area covered with geometry (d) at 700 °C will be less than the total area covered with geometry (b) at 20 °C because both have the same oxygen uptake, the difference in area of the uncovered region which affects the LEED pattern and the surface states could be somewhat compensated by the difference in strength of the rearrangement. In other words, the same amount of distortion or rearrangement of the clean 7×7 surface is possibly caused by a smaller area of geometry (d) than (b).

According to the above discussion, the 1×1 LEED pattern is not due to a relaxed, ordered surface structure with bulklike 1×1 periodicity, but rather due to a disordered, amorphouslike surface structure, which has destroyed the 7×7 surface periodicity and allows one to see the 1×1 periodicity of the underlying bulk. Similarly, the disappearance of surface states can be achieved by this disordered, amorphouslike surface structure not only through the oxygen termination of the surface dangling bonds, but also through the rearrangement of the surface Si atoms themselves. Finally, we notice that this disordered, amorphouslike structure is very reasonable as an intermediate stage between the ordered 7×7 reconstructed surface and the fully amorphous surface of SiO_2.

V. CONCLUSION

We have studied the initial stage of oxidation in a wide temperature range with AES, LEED, and PES of Si $2p$ and valence states. At 20 °C the fast adsorption stage which ends at 10—30 L O_2 exposure is followed by the slow adsorption stage, and there is a saturation of oxygen uptake. In the medium temperature range (300—500 °C), enhancement of oxygen uptake, instead of saturation, was observed. At 700 °C, oxygen uptake is extremely suppressed at low exposures because of desorption of oxygen as volatile SiO molecules. The intermediate 1×1 LEED pattern appears at the same oxygen amount that causes the surface states to disappear. Consequently, the 1×1 LEED pattern and the disappearance of surface states are apparently governed only by the amount of adsorbed oxygen and have no direct dependence on exposure temperature. The study of Si $2p$ chemical shifts and valence states profiles, however, indicates that atomic bonding geometries during oxidation are strongly dependent on temperature and oxidation proceeds in a somewhat phase-separated manner at high temperatures. Temperature-induced phase separation as a bulk property of SiO_x is well known. Therefore, the phase-separated oxidation observed here may be understood with the bulk phase separation. Possible atomic bonding geometries have been proposed to interpret our Si $2p$ data. Detailed interpretation of the 1×1 LEED pattern and the disappearance of surface states seems to be difficult because oxidation occurs in a nonuniform fashion. Rearrangement of the clean or less oxidized area surrounding locally oxidized area may play a key role in the formation of 1×1 LEED pattern and the disappearance of surface states. However, further study is necessary to answer this question.

ACKNOWLEDGMENTS

We gratefully acknowledge the expert experimental collaboration of P. Jupiter and H. Nakamura, as well as the careful reading of the manuscript by J. Nogami. Support for this study from Nippon Telegraph and Telephone Corporation (NTT) is gratefully acknowledged. One of the authors (M.T.) greatly appreciates Dr. H. Nomura, Dr. T. Suzuki, Dr. M. Kondo, Dr. N. Owada, and Dr. T. Sakai for having arranged his stay at Stanford from NTT.

Three of us, (T.T.C., I.L., and W.E.S.), would like to express our thanks to the Army Research Office for support under Contract No. DAAG 29-82-K0087. The experiments were performed at the Stanford Synchrotron Radiation Laboratory, which is supported by the U.S. Department of Energy (Office of Basic Energy Sciences) and by the National Science Foundation (Division of Materials Research).

[1]J. T. Law, J. Phys. Chem. Solids **4**, 91 (1958).
[2]M. Green and K. H. Maxwell, J. Phys. Chem. Solids **13**, 145 (1960).
[3]M. Green and A. Liberman, J. Phys. Chem. Solids **23**, 1407 (1962).
[4]H. Ibach, K. Horn, R. Dorn, and H. Lüth, Surf. Sci. **38**, 433 (1973).
[5]F. Meyer and J. J. Vrakking, Surf. Sci. **38**, 275 (1973).
[6]H. Ibach and J. E. Rowe, Phys. Rev. B **10**, 710 (1974).
[7]R. Ludeke and A. Koma, Phys. Rev. Lett. **34**, 1170 (1975).
[8]G. Margaritondo, J. E. Rowe, and S. B. Christman, Nuovo Cimento Soc. Ital. Fis. B **39**, 781 (1977).
[9]C. M. Garner, I. Lindau, C. Y. Su, P. Pianetta, and W. E. Spicer, Phys. Rev. B **19**, 3944 (1979).
[10]H. Ibach, H. D. Bruchmann, and H. Wagner, Appl. Phys. A **29**, 113 (1982).
[11]G. Hollinger and F. J. Himpsel, Phys. Rev. B **28**, 3651 (1983).
[12]C. Y. Su, P. R. Skeath, I. Lindau, and W. E. Spicer, J. Vac. Sci. Technol. **19**, 481 (1981).
[13]G. Hollinger, Y. Jugnet, and Tran Minh Duc, Solid State Commun. **22**, 277 (1977).
[14]W. E. Spicer, J. Phys. (Paris) Colloq. **34**, C6-19 (1973).
[15]J. J. Lander and J. Morrison, J. Appl. Phys. **33**, 2089 (1962).
[16]C. Gelain, A. Cassuto, and P. Le Goff, Oxid. Met. **3**, 139 (1971).
[17]L. F. Wagner and W. E. Spicer, Phys. Rev. Lett. **28**, 1381 (1972); L. F. Wagner, Ph.D. thesis, Stanford University, 1981.
[18]F. J. Himpsel, P. Heimann, T. C. Chiang, and D. E. Eastman, Phys. Rev. Lett. **45**, 1112 (1980).
[19]S. Brennan, J. Stöhr, R. Jaeger, and J. E. Rowe, Phys. Rev. Lett. **45**, 1414 (1980).
[20]F. J. Grunthaner, P. J. Grunthaner, R. P. Vasquez, B. F. Lewis, J. Maserjian, and A. Madhukar, Phys. Rev. Lett. **43**, 1683 (1979).
[21]F. J. Grunthaner, P. J. Grunthaner, R. P. Vasquez, B. F. Lewis, J. Maserjian, and A. Madhukar, J. Vac. Sci. Technol. **16**, 1443 (1979).
[22]G. Hollinger and F. J. Himpsel, J. Vac. Sci. Technol. A **1**, 640 (1983).
[23]G. Hollinger and F. J. Himpsel, Phys. Rev. B **28**, 3651 (1983).
[24]G. Hollinger and F. J. Himpsel, Appl. Phys. Lett. **44**, 93 (1984).
[25]S. T. Pantelides and W. A. Harrison, Phys. Rev. B **13**, 2667 (1976).
[26]S. Ciraci, S. Ellialtioğlu, and S. Erkoc, Phys. Rev. B **26**, 5716 (1982).
[27]M. Lannoo and G. Allan, Solid State Commun. **28**, 733 (1978).
[28]C. R. Helms, N. M. Johnson, S. A. Schwarz, and W. E. Spicer, J. Appl. Phys. **50**, 7007 (1979).
[29]T. H. Di Stefano, J. Vac. Sci. Technol. **13**, 856 (1976).